



On the Asymptotic Behavior of Dilution Parameters for Gaussian and Hole–Gaussian Log-Conductivity Covariance Functions

MARILENA PANNONE^{1,*} and PETER K. KITANIDIS²

¹*Dipartimento di Ingegneria e Fisica dell'Ambiente, Università della Basilicata, Potenza, Italy*

²*Department of Civil and Environmental Engineering, Stanford University, Stanford, CA, USA*

(Received: 6 December 2002; in final form: 6 August 2003)

Abstract. Using a Lagrangian approach, the authors have previously shown that the kinetics of concentration variance and dilution of passive solutes in heterogeneous aquifers depend on the ratio between two- and one-particle covariances. Extending this approach, it is here demonstrated that, for point injections, the two-particle covariance coincides with the variance of the centroid location. Then, based on an Eulerian formulation, analytical first-order approximations are obtained for the two-particle covariance, for two types of log-conductivity covariance. For Gaussian covariance functions, whereas the transverse moments are asymptotically constant, the longitudinal moment tends to increase logarithmically over time. For hole–Gaussian covariances, both transverse and longitudinal moments tend to constant values. In both cases, the longitudinal two-particle correlation, which plays a crucial role in determining the dynamics of the concentration fluctuations, is controlled by the magnitude of the local dispersivity. The theoretical predictions are compared to the data collected at the Cape Cod site in terms of time derivative of the longitudinal two-particle moment, for Gaussian log-conductivity covariance and resorting to maximum likelihood estimates. Generally, good agreement is there, between experimental data and analytical expressions.

Key words: two- and one-particle covariances, characteristic dilution times, analytical derivation, concentration spatial structure, maximum likelihood estimates, comparison with field measurements.

1. Introduction

It is well understood that the pronounced nonuniformity of groundwater velocity, due to the heterogeneity of the geologic formations, is primarily responsible in the long term for the spreading of solutes in aquifers. There has been considerable research on field-scale transport in porous media characterized by translational invariance, such as stratified, periodic, and stationary media. Field-scale transport is described through a mean concentration that satisfies the advection–dispersion equation with constant mean velocity \mathbf{U} and large-time macrodispersion tensor \mathbf{D}_m (Gelhar and Axness, 1983; Dagan, 1984, 1989; Güven *et al.*, 1984; Neuman *et al.*, 1987; Rubin, 1990; Kitanidis, 1992). However, the mean concentration, viewed as an ensemble mean or as a spatial average, is a smoothed version of the actual

*Author for correspondence: E-mail: pannone@unibas.it

one. In many groundwater pollution problems, one needs to determine whether the concentration of dissolved chemicals meets a quality standard and must thus evaluate the difference between the actual and the mean distributions.

A suitable measure of the expected deviation is the concentration variance. Several works (Vomvoris and Gelhar, 1990; Kapoor and Gelhar, 1994a, b; Kapoor and Kitanidis, 1998; Pannone and Kitanidis, 1999) have pointed out that local dispersion plays a crucial role in determining the behavior over time of concentration variance and coefficient of variation. In particular, Pannone and Kitanidis (1999) have used a large-time Lagrangian approach to show that the kinetics of concentration variance and dilution depend on the ratio between two- and one-particle covariances. The smaller the ratio, the more diluted the plume. The one-particle covariance is the tensor of the mean square deviation of the location of a single particle from its mean:

$$X_{ij} = \langle X'_i X'_j \rangle = \langle X_i X_j \rangle - \langle X_i \rangle \langle X_j \rangle \quad (1)$$

where X_i is the i th component of the particle position vector; the angle brackets indicate the ensemble average, and $X'_i = X_i - \langle X_i \rangle$. The two-particle covariance is the covariance tensor of the locations of two particles that, started from the same point, follow different paths due to the Brownian motion:

$$\Theta_{ij} = \langle X'_i Y'_j \rangle = \langle X_i Y_j \rangle - \langle X_i \rangle \langle Y_j \rangle \quad (2)$$

In the above expression, Y indicates the coordinates of the second particle.

The Lagrangian theory of Dagan (1984) extended by Fiori (1996) to finite-Peclet cases, as well as the numerical experiments by Bellin *et al.* (1992) and the Eulerian theory of Gelhar and Axness (1983), predict that the one-particle covariances increase linearly in time, at large times and in stationary formations. On the other hand, Pannone and Kitanidis (1999) suggest that Θ_{ij} should increase more slowly than X_{ij} and may tend to become constant; they also demonstrate that the large-time Θ_{ij} goes to constant for confined stratified formations. Some interesting theoretical analyses of the two-particle correlation in turbulent fluid fields have been presented by Batchelor (1952) and by Fisher *et al.* (1979). More recently, Fiori and Dagan (2000) have studied the two-particle moments for generally nonpoint solute sources and exponential log-conductivity through a first-order Lagrangian approach.

Here, the time behavior of Θ_{ij} is analyzed in the case of porous formations characterized by classic stationary and hole-type log-conductivity covariance functions. First, the two-particle moments are expressed in terms of hierarchical ensemble averages leading to an important relation between the two-particle covariance and the variance of the centroid of the 'single-realization' plume. This relation is important not only because it gives valuable insights on how two seemingly different quantities are related, but also because many interesting conclusions can be drawn. Next, an Eulerian-Lagrangian approach is developed for the determination of Θ_{ij} in transient and asymptotic conditions, and the general differential equations are

solved for Gaussian and first type hole-Gaussian log-conductivity covariances. Finally, the longitudinal two-particle moments are derived as maximum likelihood estimates from the concentration data collected during the late sampling rounds of the Cape Cod tracer test, and are compared to the analytical predictions in terms of rates of change over time.

2. Hierarchical Ensemble Averaging

The ensemble mean operation indicated by angle brackets in Equations (1) and (2) can be broken up into two hierarchical operations: the first operation, E_1 , is to take the ensemble mean over all the possible realizations of the Brownian displacements conditional on a realization of the velocity field; the second operation, E_2 , is to take the ensemble mean over all the realizations of the random velocity field. Note that $E_1[X_i]$ is the i th component of the centroid position vector for a unit normalized mass of solute instantaneously injected at a point of a single realization of the velocity field.

Using a well-known relation from probability theory, also used in Kitanidis (1988) and Dagan (1990), we can write:

$$X_{ij} = \langle X'_i X'_j \rangle = E_2 \{ E_1 [(X_i - E_1(X_i))(X_j - E_1(X_j))] \} + E_2 \{ (E_1(X_i) - \langle X_i \rangle)(E_1(X_j) - \langle X_j \rangle) \} \quad (3)$$

Considering an ensemble of plumes, one for each realization of the velocity field, the first term on the right-hand side is the average second spatial moment of the plumes, denoted by S_{ij} , and the second term is the covariance of the centroids, denoted by \mathcal{U}_{ij} . The average second spatial moment has been studied as a measure of spreading by Dagan (1991, 1994), Rajaram and Gelhar (1993), Dentz *et al.* (2000a, b); they used its time rate of increase to define a macrodispersivity that is dependent on the plume scale.

The same formulation can be used for the two-particle covariance:

$$\Theta_{ij} = \langle X'_i Y'_j \rangle = E_2 \{ E_1 [(X_i - E_1(X_i))(Y_j - E_1(Y_j))] \} + E_2 \{ (E_1(X_i) - \langle X_i \rangle)(E_1(Y_j) - \langle Y_j \rangle) \} \quad (4)$$

In a given realization, the trajectories of two particles started at the same time from the same point have the same probability distribution, which means that the second term on the right-hand side is \mathcal{U}_{ij} ; knowledge of the location of one particle does not change the pdf of the other particle, which means that the single-realization displacements of the two particles are independent and thus the first term on the right-hand side vanishes. Thus we obtain a useful relation:

$$\Theta_{ij} = \mathcal{U}_{ij} \quad (5)$$

That is, for the case of instantaneous point injection and unit total mass, the two-particle covariance is identical to the centroid covariance.

Combining (5) and (3), we obtain:

$$\langle S_{ij} \rangle = \langle X'_i X'_j \rangle - \langle X'_i Y'_j \rangle \quad (6)$$

Thus, the ensemble second spatial moment can be expressed as the difference between the one- and two-particle covariances. Since the ensemble second spatial moment is positive and increasing, it is clear that the one-particle covariance always increases faster than the two-particle covariance.

3. Analytical Formulation

The starting basis for the derivation of the two-particle moments is represented by the advection–dispersion equation in its simplest multi-dimensional form:

$$\frac{\partial c}{\partial t} + \mathbf{u} \cdot \nabla c - \nabla \cdot (\mathbf{D} \nabla c) = 0 \quad (7)$$

Here, c is the aqueous-phase concentration due to instantaneous point injection of a solute in $\mathbf{x} = 0$ at $t = 0$, $\mathbf{u} = \mathbf{u}(\mathbf{x})$ is the solenoidal velocity field, and \mathbf{D} is the local dispersion tensor. We are primarily interested at time-rates of change at large times, when the diffusion length, of order \sqrt{Dt} (with D representative local dispersion coefficient), has become much larger than the heterogeneity correlation length I_Y and the plume has lost the ‘memory’ of the initial conditions. Hence, the initial condition is only a simplification that involves no loss of generality. Also, we focus on purely local approaches and on cases of mild heterogeneity envisioned in the methods of Dagan (1989), Gelhar (1997), Rubin (2003). The study of large-time transport processes is practically useful because of the large times involved in transport of chemicals in groundwater and the need for predictive models over large time scales.

Because of (5), the determination of the two-particle covariance is equivalent to the determination of the centroid covariance in case of instantaneous point injection and unit total mass. Thus, as a first step, we multiply each term of (7) by x_i and we integrate over the whole unbounded flow domain in order to obtain the governing equation of the time-dependent centroid position vector. As in Kitanidis (1988), Dagan (1990) and others, we obtain:

$$\frac{dR_i}{dt} = \frac{d\langle R_i \rangle}{dt} + \frac{dR'_i}{dt} = U_i + \int u'_i(\mathbf{x}) c(\mathbf{x}, t) d\mathbf{x} \quad (8)$$

Here, $R_i(t) = \int x_i c(\mathbf{x}, t) d\mathbf{x}$ is the i th component of the centroid position vector, $U_i = \langle u_i(\mathbf{x}) \rangle$ is the i th component of the mean velocity, and $u'_i = u_i - U_i$. We assumed that c and its spatial derivatives vanish at the edges of the very large domain.

In a reference frame whose axes are aligned with the plume isotropy–anisotropy principal directions, the two-particle covariance is given by

$$\Theta_{ii} = \mathcal{U}_{ii} = \langle R_i'^2 \rangle \quad i = 1, \dots, n \quad (9)$$

where n is the dimensionality of the flow domain. It can be shown that, at leading order in terms of $\log-K$ or velocity variation, the expected value of $\int u'_i(\mathbf{x})c(\mathbf{x}, t) d\mathbf{x}$ is zero. For illustration, we will employ the well-known local Eulerian relation (Gelhar and Axness, 1983) that gives, at lowest order:

$$\langle u'_i(\mathbf{x})c(\mathbf{x}, t) \rangle = -D_{a ii}(t) \frac{\partial \langle c(\mathbf{x}, t) \rangle}{\partial x_i} \quad (10)$$

where $D_{a ii}(t)$ indicates the advection-controlled portion of the macrodispersion coefficient ($D_{m ii} = D_{a ii} + D_{ii}$). Because of the concentration–mean boundary conditions ($\langle c(\mathbf{x}, t) \rangle \rightarrow 0$ when $x_i \rightarrow \pm \infty$), one obtains:

$$\left\langle \int u'_i(\mathbf{x})c(\mathbf{x}, t) d\mathbf{x} \right\rangle = \int \langle u'_i(\mathbf{x})c(\mathbf{x}, t) \rangle d\mathbf{x} = -D_{a ii}(t) \int \frac{\partial \langle c(\mathbf{x}, t) \rangle}{\partial x_i} d\mathbf{x} = 0 \quad (11)$$

Thus,

$$\frac{d\langle R_i \rangle}{dt} = U_i \quad \text{or} \quad \langle R_i \rangle = U_i t \quad (12)$$

and

$$\frac{dR'_i}{dt} = \int u'_i(\mathbf{x})c(\mathbf{x}, t) d\mathbf{x} \quad \text{or} \quad R'_i(t) = \int_0^t \int u'_i(\mathbf{x})c(\mathbf{x}, \tau) d\mathbf{x} d\tau \quad (13)$$

Now, since

$$\frac{dR_i'^2}{dt} = 2R'_i \frac{dR'_i}{dt} \quad (14)$$

the two-particle covariance will be computed from

$$\begin{aligned} \frac{d\Theta_{ii}}{dt} &= 2 \left\langle R'_i \frac{dR'_i}{dt} \right\rangle \\ &= 2 \left\langle \int_0^t \int \int u'_i(\mathbf{x})u'_i(\mathbf{y})c(\mathbf{x}, t)c(\mathbf{y}, \tau) d\mathbf{x} d\mathbf{y} d\tau \right\rangle \end{aligned} \quad (15)$$

The early Lagrangian approaches (e.g. Dagan, 1984) dealt with the transport problem for $Pe = \infty$, that is, negligible local dispersion; furthermore, assuming that the stationary log-conductivity field was only weakly heterogeneous, and in order to solve the trajectory integro-differential equation, they considered the advective fluctuation very small as compared to the mean displacement and therefore negligible. In that case, the solute concentration due to a unit normalized mass injected into a small cube of volume V_0 centered at the origin of the reference frame is given by

$$c(\mathbf{x}, t) = \int_{V_0} C_0(\mathbf{a})\delta(\mathbf{x} - \mathbf{a} - \mathbf{U}t) d\mathbf{a} \quad (16)$$

where the initial distribution is $C_0(\mathbf{a}) \rightarrow \delta(\mathbf{a})$ and $\delta(\bullet)$ indicates, as usual, the Dirac delta function. By substituting (16) into (15), we obtain:

$$\frac{d\Theta_{ii}}{dt} = 2 \int_0^t \langle u'_i(\mathbf{U}t) u'_i(\mathbf{U}\tau) \rangle d\tau = 2 \int_0^t C_{iii}[\mathbf{U}(t - \tau)] d\tau \quad (17)$$

which is exactly the same differential equation holding for the derivative of the one-particle covariance (Dagan, 1984). Note that, in (17) and in what follows, $C_{iii}(\mathbf{x} - \mathbf{y}) = \langle u'_i(\mathbf{x}) u'_i(\mathbf{y}) \rangle$ represents the covariance function of the stationary Eulerian velocity field. However, such an assumption, which dramatically simplifies the formulation and the corresponding solution, is unsuitable except at very short times, when the scattering of particles is still very limited.

A definite improvement is represented by the assumption that the particles move along the mean trajectory perturbed by Brownian displacements only (e.g. Fiori, 1996; Fiori and Dagan, 2000). In this case, the particle sampling domain is correctly multi-dimensional and increasing over time, although at a rate that does not match the macrodispersive contribution. The corresponding concentration is given by

$$c(\mathbf{x}, t) = \int_{V_0} C_0(\mathbf{a}) \delta[\mathbf{x} - \mathbf{a} - \mathbf{U}t - \mathbf{X}_B(t)] d\mathbf{a} \quad (18)$$

where, again, $C_0(\mathbf{a}) \rightarrow \delta(\mathbf{a})$ and \mathbf{X}_B is the normally distributed local-dispersive displacement. Thus,

$$\begin{aligned} \frac{d\Theta_{ii}}{dt} &= 2 \left\langle \int_0^t \int \int u'_i(\mathbf{x}) u'_i(\mathbf{y}) \delta[\mathbf{x} - \mathbf{U}t - \mathbf{X}_B(t)] \delta[\mathbf{y} - \mathbf{U}\tau - \mathbf{Y}_B(\tau)] d\mathbf{x} d\mathbf{y} d\tau \right\rangle \\ &= 2 \int_0^t \int \int \langle u'_i(\mathbf{x}) u'_i(\mathbf{y}) \rangle \delta[\mathbf{x} - \mathbf{U}t - \mathbf{X}_B(t)] \delta[\mathbf{y} - \mathbf{U}\tau - \mathbf{Y}_B(\tau)] d\mathbf{x} d\mathbf{y} d\tau \\ &= 2 \int_0^t \int \int \int \langle u'_i(\mathbf{x}) u'_i(\mathbf{y}) \rangle \delta[\mathbf{x} - \mathbf{U}t - \mathbf{X}_B(t)] \delta[\mathbf{y} - \mathbf{U}\tau - \mathbf{Y}_B(\tau)] \cdot \\ &\quad \cdot f_{\mathbf{X}_B \mathbf{Y}_B}(\mathbf{X}_B, \mathbf{Y}_B; t, \tau, Pe) d\mathbf{x} d\mathbf{y} d\mathbf{X}_B d\mathbf{Y}_B d\tau \end{aligned} \quad (19)$$

where $f_{\mathbf{X}_B \mathbf{Y}_B}(\mathbf{X}_B, \mathbf{Y}_B; t, \tau, Pe)$ is the joint probability density function of two different Brownian trajectories. Note that, in the third line of the above equation, the statistical independence of advective velocity and diffusive displacements allows for subdividing the global ensemble mean into two nonsequential averaging operations. Moreover, since the Brownian displacements of two different particles are uncorrelated at any time by definition, we have:

$$\begin{aligned} f_{\mathbf{X}_B \mathbf{Y}_B}(\mathbf{X}_B, \mathbf{Y}_B; t, \tau, Pe) &= f_{\mathbf{X}_B}(\mathbf{X}_B; t, Pe) f_{\mathbf{Y}_B}(\mathbf{Y}_B; \tau, Pe) \\ &= \prod_{r=1}^n \frac{1}{\sqrt{4\pi D_{rr}t}} \frac{1}{\sqrt{4\pi D_{rr}\tau}} \exp \left[-\frac{X_{B,r}^2}{4D_{rr}t} \right] \cdot \\ &\quad \cdot \exp \left[-\frac{Y_{B,r}^2}{4D_{rr}\tau} \right] \end{aligned} \quad (20)$$

where \prod indicates the product over the different components.

From (19), by performing the integrations over \mathbf{X}_B and \mathbf{Y}_B :

$$\frac{d\Theta_{ii}}{dt} = 2 \int_0^t \int \int C_{iii}(\mathbf{x} - \mathbf{y}) \cdot f_{\mathbf{X}_B \mathbf{Y}_B}(\mathbf{x} - \mathbf{U}t, \mathbf{y} - \mathbf{U}\tau; t, \tau, Pe) d\mathbf{x} d\mathbf{y} d\tau \quad (21)$$

or

$$\Theta_{ii}(t) = \int_0^t \int_0^t \int \int C_{iii}(\mathbf{x} - \mathbf{y}) \cdot f_{\mathbf{X}_B \mathbf{Y}_B}(\mathbf{x} - \mathbf{U}t_1, \mathbf{y} - \mathbf{U}t_2; t_1, t_2, Pe) d\mathbf{x} d\mathbf{y} dt_1 dt_2 \quad (22)$$

It is worth noting that, following the present Eulerian approach, there is no need for introducing specific hypotheses about the characteristics of the two-particle Lagrangian velocity correlation (which is nonstationary, as pointed out by Pannone and Kitanidis, 1999).

In the Fourier domain, the expression of the velocity covariance is:

$$C_{iii}(\mathbf{x} - \mathbf{y}) = \int_{\mathbf{k}} S_{iii}(\mathbf{k}) \exp[j2\pi \mathbf{k} \cdot (\mathbf{x} - \mathbf{y})] d\mathbf{k} \quad (23)$$

where S_{iii} indicates the velocity spectral density, \mathbf{k} is the vector of wave numbers and $j = \sqrt{-1}$. The substitution of (23) into (22) yields:

$$\Theta_{ii}(t) = \int_{\mathbf{k}} \int_0^t \int_0^t \int \int S_{iii}(\mathbf{k}) \exp[j2\pi \mathbf{k} \cdot (\mathbf{x} - \mathbf{y})] \cdot f_{\mathbf{X}_B \mathbf{Y}_B}(\mathbf{x} - \mathbf{U}t_1, \mathbf{y} - \mathbf{U}t_2; t_1, t_2, Pe) d\mathbf{x} d\mathbf{y} dt_1 dt_2 d\mathbf{k} \quad (24)$$

Finally, from (24) and (20), the integrations over \mathbf{x} and \mathbf{y} and the double integration over time lead to:

$$\Theta_{ii}(t) = \int_{\mathbf{k}} \frac{S_{iii}(\mathbf{k}) \Psi(\mathbf{k}, t)}{(2\pi \mathbf{U} \cdot \mathbf{k})^2 + [4\pi^2 (\sum_r D_{rr} k_r^2)]^2} d\mathbf{k} \quad (25)$$

where the space-time-dependent kernel $\Psi(\mathbf{k}, t)$ has the following expression:

$$\Psi(\mathbf{k}, t) = 1 + \exp \left[-8\pi^2 \left(\sum_r D_{rr} k_r^2 \right) t \right] - 2 \cos(2\pi \mathbf{U} \cdot \mathbf{k}t) \exp \left[-4\pi^2 \left(\sum_r D_{rr} k_r^2 \right) t \right] \quad (26)$$

Ideally, one should solve (15) for

$$c(\mathbf{x}, t) = \int_{V_0} C_0(\mathbf{a}) \delta[\mathbf{x} - \mathbf{a} - \mathbf{U}t - \mathbf{X}'(t, \mathbf{a})] d\mathbf{a} \quad (27)$$

where $\mathbf{X}'(t, \mathbf{a})$ is the *total* trajectory fluctuation, expression of the synergy of advection and local dispersion, which can be not negligible at large time even for weak heterogeneity (Pannone and Kitanidis, 1999). However, in this case it would not be possible to separate $\langle c(\mathbf{x}, t)c(\mathbf{y}, \tau) \rangle$ from the Eulerian velocity covariance in Equation (15) and to obtain an analytical solution without additional assumptions ($\mathbf{X}'(t, \mathbf{a})$ does depend on the advective velocity fluctuations in an intrinsically nonlinear fashion). A quasi-linear analytical solution for the one-particle moments based on the Corrsin's conjecture was proposed by Neuman *et al.* (1987).

The two-particle moments have a simple interpretation in terms of large-time concentration variance.

Let us rewrite the analytical expression of the concentration variance derived by Pannone and Kitanidis (1999) through an asymptotic Lagrangian approach as a function of the correlation coefficients $\rho_i = \Theta_{ii}/X_{ii}$, where $X_{ii} \rightarrow 2D_{mii}t$:

$$\begin{aligned} \sigma_c^2 &= \langle c^2 \rangle - \langle c \rangle^2 \\ &\rightarrow \prod_{i=1}^n \frac{1}{\sqrt{[1 - \rho_i^2(t)]}} \frac{1}{4\pi D_{mii}t} \exp \left\{ - \frac{(x_i - U_i t)^2 [1 - \rho_i(t)]}{4D_{mii}t [1 + \rho_i(t)]} \right\} \cdot \\ &\quad \cdot \exp \left[- \frac{(x_i - U_i t)^2}{4D_{mii}t} \right] - \prod_{i=1}^n \frac{1}{4\pi D_{mii}t} \exp \left[- \frac{(x_i - U_i t)^2}{2D_{mii}t} \right] \end{aligned} \quad (28)$$

We are interested in what happens when Θ_{ii} is so small compared to X_{ii} that $\rho_i \rightarrow 0$. Thus, we will expand σ_c^2 about $\boldsymbol{\rho} = (\rho_1, \dots, \rho_n) = \mathbf{0}$:

$$\sigma_c^2(\boldsymbol{\rho}) \simeq \sigma_c^2(\mathbf{0}) + \sum_{i=1}^n \left[\frac{\partial \sigma_c^2}{\partial \rho_i} \right]_{\rho_i=0} \rho_i + \dots \quad (29)$$

From (28), it is easy to show that $\sigma_c^2(\mathbf{0}) = 0$. Additionally,

$$\left[\frac{\partial \sigma_c^2}{\partial \rho_i} \right]_{\rho_i=0} = \langle c \rangle^2 \frac{(x_i - U_i t)^2}{2D_{mii}t} \quad (30)$$

Thus,

$$\sigma_c^2(\boldsymbol{\rho}) \simeq \langle c \rangle^2 \sum_{i=1}^n \frac{(x_i - U_i t)^2}{2D_{mii}t} \rho_i = \langle c \rangle^2 \sum_{i=1}^n \frac{(x_i - U_i t)^2}{(2D_{mii}t)^2} \Theta_{ii}(t) \quad (31)$$

On the other hand, the square of the derivative of the ensemble mean concentration is given by

$$\left[\frac{\partial \langle c \rangle}{\partial x_i} \right]^2 = \langle c \rangle^2 \frac{(x_i - U_i t)^2}{(2D_{mii}t)^2} \quad (32)$$

Then, at very large times we can write:

$$\sigma_c^2 = \langle c^2 \rangle \simeq \sum_{i=1}^n \Theta_{ii}(t) \left[\frac{\partial \langle c \rangle}{\partial x_i} \right]^2 \quad (33)$$

It turns out that the two-particle moments are generally time-dependent coefficients that bring forth the concentration variance just by re-scaling the square of the derivative of the ensemble mean concentration: they are important constitutive parameters that relate the large-scale variability represented by the derivatives of the ensemble mean concentration with a measure of the microscale fluctuation (see also Kapoor and Gelhar, 1994b). Given the two-particle covariances, Equation (33) is a convenient formula for the approximate estimation of the large-time concentration variance.

It is interesting to note the similarity between (33) and the expression of the turbulent velocity correlation as derived through Prandtl's theory. For instance, in case of steady 2D flow with mean velocity directed along x_1 , one has:

$$\langle v'_1 v'_2 \rangle \simeq l^2 \left(\frac{d\langle v_1 \rangle}{dx_2} \right)^2$$

where l is the mixing length. Thus, in terms of concentration variance, the square root of the two-particle moments plays the same role that the mixing length plays in terms of turbulent velocity correlation.

4. Isotropic Gaussian and Hole-Gaussian Log-Conductivity Covariance Functions

The analytical derivation of the two-particle moments for isotropic Gaussian and Hole-Gaussian log-conductivity covariance functions, and isotropic local dispersion, is relegated in Appendices A and B, respectively. See Zhang and Di Federico (1998) for the evaluation of the one-particle moments tensor in case of Gaussian covariance and $Pe \rightarrow \infty$.

For the Gaussian case, represented by the following covariance function:

$$C_Y(r)_{r=|\mathbf{r}|} = \sigma_Y^2 \exp\left(-\frac{|\mathbf{r}|^2}{l_Y^2}\right) \quad (34)$$

where $l_Y = 2I_Y/\sqrt{\pi}$ is the range of the distribution, I_Y is the integral scale, σ_Y^2 the variance, and \mathbf{r} the vector distance between two generic points, the short-time limits in case of large Peclet numbers are:

$$\Theta_{11}(t) = \frac{8}{15}\sigma_Y^2 U^2 t^2, \quad \Theta_{22}(t) = \Theta_{33}(t) = \frac{1}{15}\sigma_Y^2 U^2 t^2 \quad (35)$$

with $\mathbf{U} = (U, 0, 0)$. Note that they are the same limits found under identical conditions for the one-particle moments with exponential log-conductivity covariance (Dagan, 1984). Indeed, at short times the effect of a weak local dispersion is still negligible, and the two particles are close to each other within a very small heterogeneity sampling volume.

At large times ($\tau/Pe = (tU/I_Y)/(UI_Y/D) = Dt/I_Y^2 \rightarrow \infty$), we obtain:

$$\Theta_{11} = \frac{8Pe}{3\pi^2} \sigma_Y^2 I_Y^2 \ln \left(\frac{tU}{I_Y} \right) + \text{const}, \quad \Theta_{22} = \text{const}, \quad \Theta_{33} = \text{const} \quad (36)$$

The result is in qualitative agreement with the one predicted by Fiori and Dagan (2000) in case of exponential log-conductivity fields. Finally, for large Peclet numbers,

$$\Theta_{22} = \Theta_{33} = \frac{2}{3\pi} \sigma_Y^2 I_Y^2 \quad (37)$$

The first-type hole–Gaussian log-conductivity covariance is (Vomvoris and Gelhar, 1990):

$$C_Y(r)_{r=|\mathbf{r}|} = \frac{\sigma_Y^2}{2} \exp \left(-\frac{|\mathbf{r}|^2}{2l^2} \right) - \frac{|\mathbf{r}|^2}{6l^2} \sigma_Y^2 \exp \left(-\frac{|\mathbf{r}|^2}{2l^2} \right) \quad (38)$$

where l indicates the heterogeneity characteristic length.

In case of large Peclet numbers, at short times we obtain:

$$\Theta_{11}(t) = \frac{4}{15} \sigma_Y^2 U^2 t^2, \quad \Theta_{22}(t) = \Theta_{33}(t) = \frac{1}{30} \sigma_Y^2 U^2 t^2 \quad (39)$$

while the asymptotic values are given by

$$\Theta_{11} = \frac{\sqrt{\pi} Pe}{6\sqrt{2}} \sigma_Y^2 l^2, \quad \Theta_{22} = \Theta_{33} = \frac{\sigma_Y^2 l^2}{18} \quad (40)$$

where $Pe = Ul/D = l/\alpha$, with α local dispersivity. Thus, the main difference between the two-particle covariances obtained for Gaussian log-conductivity and the two-particle covariances obtained for hole–Gaussian log-conductivity is represented by the large-time behavior of the longitudinal moment. In the first case, it is increasing without bound over time even for finite Peclet (note that we have obtained (36) for $\tau/Pe \rightarrow \infty$); in the second case, it goes to a constant proportional to the Peclet number. It is then clear that, unlike the one-particle case, the two-particle correlation is critically controlled by the low-wave number tail of the Eulerian velocity spectrum, and a right characterization of the log-conductivity spatial distribution is extremely important in order to model the evolution of the concentration field.

For the sake of completeness, we have computed the asymptotic longitudinal, transverse and vertical macrodispersion coefficients for the hole–Gaussian log K covariance and, therefore, the asymptotic correlation coefficients (see Appendix C). For large Peclet the results are:

$$\begin{aligned} D_{m11} &= \frac{\sqrt{2\pi}}{6} \sigma_Y^2 Ul, & \rho_1 &= \frac{\Theta_{11}}{2D_{m11}t} = \frac{l^2}{4Dt}, \\ D_{m22} &= D_{m33} = \frac{\sigma_Y^2 D}{6}, & \rho_2 = \rho_3 &= \frac{\Theta_{22,33}}{2D_{m22,33}t} = \frac{l^2}{6Dt} \end{aligned} \quad (41)$$

Thus, the correlation coefficients increase with the log-conductivity correlation distance and decrease with local dispersion. It is worth noting that they turn out to be proportional to the ratio between the square of the heterogeneity characteristic length and the square of the diffusion length (which is proportional to \sqrt{Dt}). This specific rate of decay of the correlation coefficients would lead to a rate of decay of the concentration coefficient of variation at the plume center (Kapoor and Gelhar, 1994a, b; Pannone and Kitanidis, 1999) that is qualitatively similar to the one obtained by Pannone and Kitanidis (1999) for a confined stratified formation. In particular:

$$\left[\frac{\sigma_c}{\langle c \rangle} \right]_{\text{center}} \sim \frac{\tau_d}{t}$$

where τ_d , the dilution time,

$$\tau_d = \frac{1}{8} \sqrt{\left(\frac{\Theta_{11}}{D_{m11}} \right)^2 + \left(\frac{\Theta_{22}}{D_{m22}} \right)^2 + \left(\frac{\Theta_{33}}{D_{m33}} \right)^2}$$

is here given by

$$\tau_d = \frac{l^2}{48D} \sqrt{17} \quad (42)$$

5. Gaussian Anisotropic Formations: Comparison with the Cape Cod Experimental Data

The asymptotic solution (36) is here extended to the case of anisotropic formations and anisotropic local dispersion in order to compare it with the large-time two-particle moments estimated from the Cape Cod concentration data through a maximum likelihood estimate procedure. We have chosen to base the whole analysis on Gaussian-like log-conductivity covariance functions and not on their exponential counterparts due to the singular behavior of the latter near the origin and to the obvious sensitivity of the concentration fluctuations dynamics to the microscale heterogeneous structure modeling (see also Kapoor and Gelhar, 1994a, b). The starting basis for that comparison is represented by the following concentration variance–covariance function, derived through a large-time Lagrangian formulation under the hypothesis of instantaneous point injection and particle trajectories jointly normally distributed (Pannone and Kitanidis, 2001):

$$\begin{aligned} Q_c(\mathbf{x}, \mathbf{y}, t) &= \langle c(\mathbf{x}, t)c(\mathbf{y}, t) \rangle - \langle c(\mathbf{x}, t) \rangle \langle c(\mathbf{y}, t) \rangle \\ &= \left(\frac{M}{\eta} \right)^2 f_{\mathbf{X}'\mathbf{Y}'}(\mathbf{x} - \mathbf{a} - \mathbf{U}t, \mathbf{y} - \mathbf{a} - \mathbf{U}t; \mathbf{Z}, \Theta) - \\ &\quad - \left(\frac{M}{\eta} \right)^2 f_{\mathbf{X}'}(\mathbf{x} - \mathbf{a} - \mathbf{U}t; \mathbf{Z}) f_{\mathbf{X}'}(\mathbf{y} - \mathbf{a} - \mathbf{U}t; \mathbf{Z}) \end{aligned} \quad (43)$$

where

$$f_{\mathbf{X}'}(\mathbf{x} - \mathbf{a} - \mathbf{U}t; \mathbf{Z}) = (2\pi)^{-n/2} |\mathbf{Z}|^{-1/2} \times \\ \times \exp \left[-\frac{1}{2} (\mathbf{x} - \mathbf{a} - \mathbf{U}t)^T \mathbf{Z}^{-1} (\mathbf{x} - \mathbf{a} - \mathbf{U}t) \right] \quad (44)$$

and

$$f_{\mathbf{X}'\mathbf{Y}'}(\mathbf{x} - \mathbf{a} - \mathbf{U}t, \mathbf{y} - \mathbf{a} - \mathbf{U}t; \mathbf{Z}, \Theta) = (2\pi)^{-n} \left| \begin{array}{cc} \mathbf{Z} & \Theta \\ \Theta^T & \mathbf{Z} \end{array} \right|^{-1/2} \cdot \\ \cdot \exp \left\{ -\frac{1}{2} [(\mathbf{x} - \mathbf{a} - \mathbf{U}t)^T (\mathbf{y} - \mathbf{a} - \mathbf{U}t)^T] \left(\begin{array}{cc} \mathbf{Z} & \Theta \\ \Theta^T & \mathbf{Z} \end{array} \right)^{-1} \begin{bmatrix} \mathbf{x} - \mathbf{a} - \mathbf{U}t \\ \mathbf{y} - \mathbf{a} - \mathbf{U}t \end{bmatrix} \right\} \quad (45)$$

are single- and two-particle trajectory probability density functions, respectively. In the above expressions, \mathbf{a} indicates the coordinate of the injection point, M the total mass and η the porosity; \mathbf{Z} is the tensor of the one-particle covariances and Θ is the tensor of the two-particle covariances; $(\cdot)^T$ indicates vector/matrix transpose. Assuming that the concentration values are normally distributed in space, and accounting for an additional random variability due to the experimental error, one can write the logarithm of the concentration probability density function, except for a constant term, as follows:

$$F = -\frac{1}{2} \ln |\mathbf{Q}_c + \mathbf{Q}_e| - \frac{1}{2} (\mathbf{z} - \langle \mathbf{c} \rangle)^T (\mathbf{Q}_c + \mathbf{Q}_e)^{-1} (\mathbf{z} - \langle \mathbf{c} \rangle) \quad (46)$$

with

$$\mathbf{Q}_c = [Q_{cij}] = [Q_c(\mathbf{x}_i, \mathbf{x}_j, t)]$$

$$\mathbf{Q}_e = [Q_{eij}] = [Q_e(\mathbf{x}_i, \mathbf{x}_j, t)]; \quad Q_e(\mathbf{x}_i, \mathbf{x}_j, t) = [\mu z(\mathbf{x}_i, t) + \nu]^2 \delta_{ij}$$

In (46), \mathbf{z} and $\langle \mathbf{c} \rangle$ indicate vector of observations and vector of corresponding unconditional Gaussian means, respectively; \mathbf{Q}_c is the theoretical covariance tensor at the observation points; \mathbf{Q}_e is the tensor of the measurement error variance and μ and ν are two constants. Some accurate consistency tests have shown that the best fit between experimental observations and *a posteriori* estimates is achieved for $\mu = 0.07$ and $\nu = 0.1$ mg/l (Pannone and Kitanidis, 2001). That is, above a lower threshold – which represents the limit of sensitivity of the measurement devices – the error increases to 7% of the measured value. Note that plausible values of μ are 0.05–0.07 (Martin Reinhart and Gary Hopkins (Stanford University), pers. comm.).

For each sampling round, total mass, centroid position vector $\mathbf{R}(t)$ and principal inertia moments $S_{ii}(t)$ had already been computed by Garabedian *et al.* (1991). We have used them in the large-time approximation (43) assuming that

$$\mathbf{R}(t) \simeq \mathbf{a} + \mathbf{U}t,$$

$$\mathbf{S}(t) = \begin{bmatrix} S_{11}(t) & 0 & 0 \\ 0 & S_{22}(t) & 0 \\ 0 & 0 & S_{33}(t) \end{bmatrix} \simeq \mathbf{Z}(t) = \begin{bmatrix} X_{11}(t) & 0 & 0 \\ 0 & X_{22}(t) & 0 \\ 0 & 0 & X_{33}(t) \end{bmatrix}$$

The original reference frame has been transformed into a principal reference frame, with the origin located on the sea level and in correspondence of the horizontal coordinates of the center of the injection volume. Finally, the values of Θ_{ii} , viewed as the unknowns of the problem, have been derived through the Gauss–Newton maximization of (46). With reference to four of the late sampling rounds of the Cape Cod tracer test, and to the longitudinal second-order moments, we have obtained:

$$\begin{aligned} t = 273 \text{ days } \mathbf{a} + \mathbf{U}t &= [115 \quad -2.1 \quad 6.6]^T \text{ m} \quad X_{11} = 196 \text{ m}^2 \quad \Theta_{11} = 157 \text{ m}^2 \\ t = 384 \text{ days } \mathbf{a} + \mathbf{U}t &= [163 \quad -14.9 \quad 8.1]^T \text{ m} \quad X_{11} = 327 \text{ m}^2 \quad \Theta_{11} = 248 \text{ m}^2 \\ t = 461 \text{ days } \mathbf{a} + \mathbf{U}t &= [197 \quad -23.5 \quad 4.6]^T \text{ m} \quad X_{11} = 372 \text{ m}^2 \quad \Theta_{11} = 258 \text{ m}^2 \\ t = 511 \text{ days } \mathbf{a} + \mathbf{U}t &= [214 \quad -33.8 \quad 4]^T \text{ m} \quad X_{11} = 405 \text{ m}^2 \quad \Theta_{11} = 288 \text{ m}^2 \end{aligned} \quad (47)$$

The Cape Cod aquifer is located in a mildly heterogeneous sand and gravel formation whose structural-hydrogeological parameters, as derived by Garabedian *et al.* (1991), Hess *et al.* (1991) and Leblanc *et al.* (1991), are here summarized:

$$\begin{aligned} \text{Log-conductivity variance } \sigma_Y^2 &= 0.24 \\ \text{Horizontal integral scale } I_{Yh} &= 2.6 \text{ m} \\ \text{Vertical integral scale } I_{Yv} &= 0.19 \text{ m} \\ \text{Mean velocity } |\mathbf{U}| &= U_1 = 0.42 \text{ m/day} \end{aligned}$$

The extension of (36) to anisotropic formations and generally anisotropic local dispersion is straightforward and based on the same steps shown in Appendix A. From (25), and a log-conductivity covariance given by

$$C_Y(\mathbf{r}) = \sigma_Y^2 \exp\left(-\frac{r_1^2}{l_{Yh}^2} - \frac{r_2^2}{l_{Yh}^2} - \frac{r_3^2}{l_{Yv}^2}\right)$$

we obtain the following linearized solution at limit for $\tau/Pe_L \rightarrow \infty$:

$$\begin{aligned} \Theta_{11}(t) &= \frac{8ePe_L\sigma_Y^2 I_{Yh}^2}{3\pi^2 \varepsilon^{3/2}} \ln\left(\frac{tU}{I_{Yh}}\right) + \text{const}, & \Theta_{22} &= \text{const}, \\ \Theta_{33} &= \text{const} \end{aligned} \quad (48)$$

where

$$\begin{aligned} I_{Yh} &= \frac{\sqrt{\pi}}{2} l_{Yh}, & I_{Yv} &= \frac{\sqrt{\pi}}{2} l_{Yv}, & \tau &= \frac{tU}{I_{Yh}}, \\ e &= \frac{I_{Yv}}{I_{Yh}}, & \varepsilon &= \frac{D_T}{D_L} = \frac{U\alpha_T}{U\alpha_L} = \frac{\alpha_T}{\alpha_L}, & Pe_L &= \frac{UI_{Yh}}{D_L} \end{aligned}$$

In terms of longitudinal two-particle moment derivative,

$$\frac{d\Theta_{11}}{dt} = \frac{8ePe_L\sigma_Y^2 I_{Y_h}^2}{3\pi^2\varepsilon^{3/2}} \frac{1}{t} \quad (49)$$

Thus, for given I_{Y_h} and α_L , the larger the local dispersion anisotropy ratio ε , the slower the logarithmic increment of Θ_{11} ; on the other hand, the larger the structural anisotropy ratio e , the faster the increment. This type of behavior makes physically sense: indeed, a large local dispersion anisotropy ratio would mean a considerable dilution along the vertical coordinate and, therefore, a faster loss of Lagrangian velocity correlation; conversely, a large value of e would correspond to a persistent ‘determinism’ of the velocity field along x_3 and, therefore, to a slower tendency towards the complete mixing.

The asymptotic values of Θ_{22} and Θ_{33} , here shown for the sake of completeness, have been computed for large Peclet numbers. At the leading order:

$$\frac{\Theta_{22}}{\sigma_Y^2 I_{Y_h}^2} = \frac{e}{2\pi} \left\{ \left[\frac{2}{\sqrt{1-e^2}} - \frac{1}{(1-e^2)^{3/2}} \right] \sin^{-1}(\sqrt{1-e^2}) + \frac{e}{1-e^2} \right\} \quad (50)$$

$$\frac{\Theta_{33}}{\sigma_Y^2 I_{Y_h}^2} = \frac{e}{\pi} \left\{ \frac{\sin^{-1}(\sqrt{1-e^2})}{(1-e^2)^{3/2}} - \frac{e}{1-e^2} \right\} \quad (51)$$

As we would expect, the horizontal transverse and the vertical two-particle covariances turn out to be usually very small and decreasing for decreasing e . At the limit for $e \rightarrow 1$, $\Theta_{22,33}/\sigma_Y^2 I_{Y_h}^2 \rightarrow 2/3\pi$ (Eq. (37)).

Despite the simplicity of equations like (50) and (51), the time needed in order to reach a stable constant behavior for the transverse covariances is very large. Thus, the comparison between analytical predictions and experimental estimates will be attempted for the longitudinal moment only.

Based on (47), and resorting to the least squares interpolation method, we can approximate the experimental behavior of Θ_{11} through the following logarithmic law:

$$\Theta_{11}^E = 198.57 \ln t - 950.2 \quad (52)$$

or, in terms of longitudinal two-particle moment derivative,

$$\frac{d\Theta_{11}^E}{dt} = \frac{198.57}{t} \quad (53)$$

In Figure (1) we have shown the fitted curve (52) and the two-particle moments derived from the experimental data. All the Θ_{11} -points fall within a 92% confidence interval. In Figure (2) we have plotted (49) for $\alpha_T = 0.001$ m and the effective

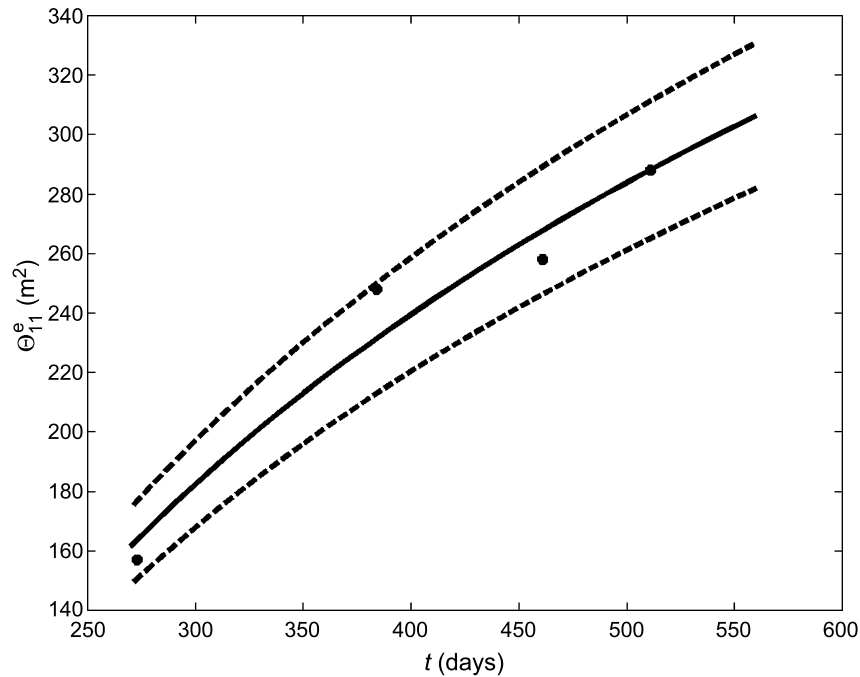


Figure 1. Longitudinal two-particle moment behavior at the Cape-Cod site. The markers indicate the experimental Θ_{11} at 273, 384, 461 and 511 days after injection; the full line represents the fitted logarithmic curve; the dashed lines represent the 92% confidence interval.

values of I_{Yh} , I_{Yv} , σ_Y^2 . We have decided to adopt this particular value of transverse local dispersivity based on the values of longitudinal, horizontal and vertical transverse dispersivity for Cape Cod data estimated by Garabedian *et al.* (1991). Given that the estimation of local dispersivity, rigorously decoupled from macroscale effects, is very complicated in field experiments, we have chosen to refer to the value of the ‘global’ vertical transverse dispersivity since, acting in a plane perpendicular to the flow, it should be almost unaffected by advection and then essentially due to local mechanisms. Garabedian *et al.* (1991) found $\alpha_T = 0.0015$ m. We slightly reduced that value in order to approximately account for possible small additional advection contributions. The local dispersion anisotropy ratio ε is allowed to vary between 0.1 and 0.4. In the same figure, we have plotted (53). As we can see, the theoretical model seems to be able to capture the effective large time-dependence of Θ_{11} ; furthermore, Equation (53) is well approximated by (49) when ε is about 0.18, that is when transverse local dispersivity is about the 18% of longitudinal local dispersivity. Thus, based on the present Lagrangian model, the large-time concentration dynamics at the Cape Cod site seems to be correctly interpreted by a local dispersion process influenced by the combined effect of diffusion and local-scale advection (which contrasts the isotropy of molecular diffusion because of a preferential flux direction).

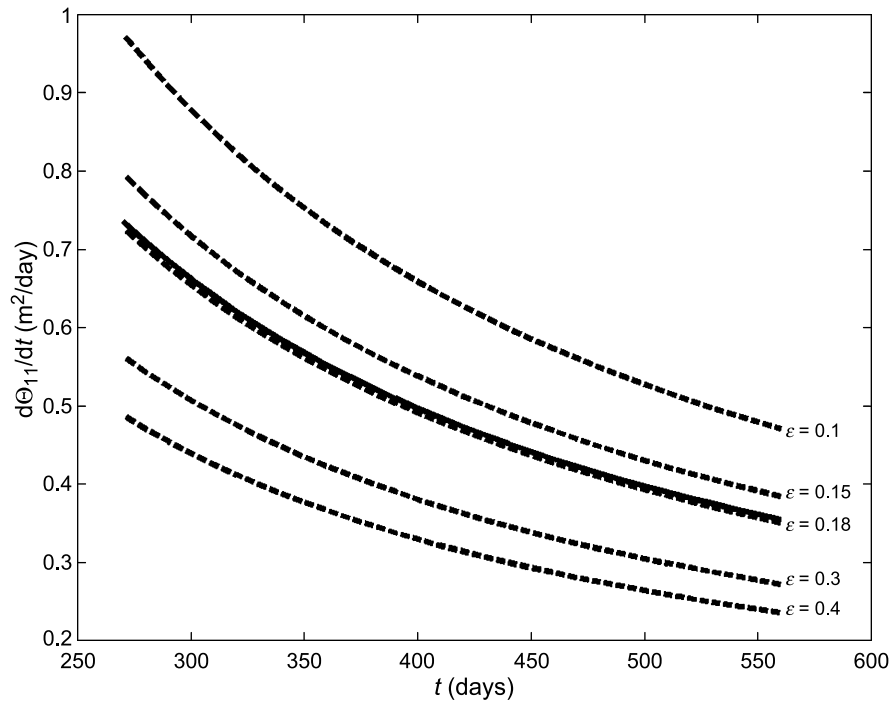


Figure 2. Longitudinal two-particle moment derivative. The full line corresponds to the fitted curve; the dashed lines correspond to the theoretical behavior for local dispersion anisotropy ratio ranging from 0.1 to 0.4.

6. Summary and Conclusions

The prediction of the location and extent of contaminant plumes, combined with the prediction of the rate with which the peaks of the concentration distribution attenuate over time, are issues of fundamental importance in hydrogeology. A previous work (Pannone and Kitanidis, 1999), based on a large-time Lagrangian approach, had shown that the ratio between the two- and one-particle covariances controls the dilution rate. The one-particle moments, and the related macrodispersion coefficients, have been the subject of several detailed studies in the recent past. In the present work, we have derived general equations as well as analytical approximations of the two-particle moments for isotropic Gaussian and hole-Gaussian log K distributions. For hole-Gaussian log-conductivity fields, it is clear that the two-particle covariances tend to constant values at large times. Thus, in this case, the coefficient of variation of the concentration at the center of the plume decreases like τ_d/t , where τ_d is a characteristic dilution time, as previously expected by Kapoor and Gelhar (1994a, b) and Pannone and Kitanidis (1999). However, for the classic Gaussian log-conductivity distributions, the leading-order approximation predicts that the longitudinal two-particle covariance increases logarithmically over time, with only its derivative tending toward zero. Nevertheless, although one

cannot define a characteristic dilution time in the way it would have been possible if the two-particle covariance had tended to become constant, this prediction means that the coefficient of variation at the center of the plume tends to zero as time tends to infinity. Moreover, the two-particle covariances have been shown to have a straightforward interpretation in terms of large-time concentration variability; indeed, they can be viewed as a kind of macro–microscale transfer functions, which transform the large-scale concentration variability represented by the spatial derivative of the concentration ensemble mean into a measure of local scale variability. In a practical situation where the transient behavior of Θ_{ii} is required in order to assess the effective plume dilution level, one could resort to the numerical integration of (25)–(26) for the given time. Note that the needed degree of accuracy in the discretization of the wave numbers domain does depend on t .

Finally, the longitudinal two-particle moments estimated from the Cape Cod concentration data have been compared to the analytical predictions in terms of large-time derivative, assuming that the log-conductivity field is represented by an anisotropic Gaussian covariance function. The results indicate that the theoretical model fits the experimental estimates reasonably well; in particular, the best agreement is achieved for large-time local dispersion represented by an anisotropy ratio $\varepsilon = 0.18$, that is, influenced by the combined effect of diffusion and small-scale advection. For a large-time predictions, knowledge – or estimation – of the concentration distribution at a certain t^* allows for the evaluation of $\Theta(t^*)$ and, therefore, for the use of Equations (48) at $t > t^*$, given the structural-hydrogeological parameters of the site. For the longitudinal covariance:

$$\begin{aligned}\Theta_{11}(t) &= \Theta_{11}(t^*) + \frac{8ePe_L\sigma_Y^2I_{Yh}^2}{3\pi^2\varepsilon^{3/2}} \ln\left(\frac{tU}{I_{Yh}}\right) - \frac{8ePe_L\sigma_Y^2I_{Yh}^2}{3\pi^2\varepsilon^{3/2}} \ln\left(\frac{t^*U}{I_{Yh}}\right) \\ &= \Theta_{11}(t^*) + \frac{8ePe_L\sigma_Y^2I_{Yh}^2}{3\pi^2\varepsilon^{3/2}} \ln\left(\frac{t}{t^*}\right)\end{aligned}$$

Appendix A.

The spectral density corresponding to (34) is:

$$\begin{aligned}S_Y(k)_{k=|\mathbf{k}|} &= \int_{\mathbf{r}} C_Y(r) \exp(-j2\pi\mathbf{k} \cdot \mathbf{r}) \, d\mathbf{r} \\ &= 8\sigma_Y^2I_Y^3 \exp(-4\pi|\mathbf{k}|^2I_Y^2)\end{aligned}\tag{A.1}$$

Furthermore, in the context of a linear formulation of the flow problem and for a 3D unbounded flow domain, the spectral density of the velocity is found through

$$S_{u_{il}}(\mathbf{k}) = \sum_{p=1}^3 \sum_{q=1}^3 U_p U_q \left(\delta_{pi} - \frac{k_i k_p}{|\mathbf{k}|^2} \right) \left(\delta_{ql} - \frac{k_l k_q}{|\mathbf{k}|^2} \right) S_Y(\mathbf{k})$$

(Gelhar and Axness, 1983), where δ is the Kronecker's Delta. The solution of (25) will be pursued under the following conditions:

$$\mathbf{U} = (U, 0, 0), \quad D_{ii} = D \quad \text{for any } i$$

That is, the x_1 -axis is aligned with the mean flow direction and local dispersion is isotropic. Then, in dimensionless terms, and after a little algebra, Equation (25) can be transformed into:

$$\begin{aligned} \frac{\Theta_{ii}}{\sigma_Y^2 I_Y^2} &= \frac{2}{\pi^2} \int_{-\infty}^{\infty} \int_{-\infty}^{\infty} \int_{-\infty}^{\infty} \frac{F_{ii}(\lambda_1, \lambda_2, \lambda_3) \exp[-4\pi(\sum_r \lambda_r^2)]}{\lambda_1^2 + (4\pi^2/Pe^2)(\sum_r \lambda_r^2)^2} \cdot \\ &\cdot \left\{ 1 + \exp\left[-\frac{8\pi^2}{Pe}\left(\sum_r \lambda_r^2\right)\tau\right] - 2 \cos(2\pi\lambda_1\tau) \times \right. \\ &\times \left. \exp\left[-\frac{4\pi^2}{Pe}\left(\sum_r \lambda_r^2\right)\tau\right] \right\} d\lambda_1 d\lambda_2 d\lambda_3 \end{aligned} \quad (\text{A.2})$$

where $\lambda_i = k_i I_Y$, $\tau = tU/I_Y$, $Pe = UI_Y/D$ and

$$\begin{aligned} F_{11}(\lambda_1, \lambda_2, \lambda_3) &= \left(1 - \frac{\lambda_1^2}{\lambda_1^2 + \lambda_2^2 + \lambda_3^2}\right)^2, \\ F_{22}(\lambda_1, \lambda_2, \lambda_3) &= \left(\frac{\lambda_1\lambda_2}{\lambda_1^2 + \lambda_2^2 + \lambda_3^2}\right)^2, \\ F_{33}(\lambda_1, \lambda_2, \lambda_3) &= \left(\frac{\lambda_1\lambda_3}{\lambda_1^2 + \lambda_2^2 + \lambda_3^2}\right)^2 \end{aligned}$$

An equivalent form of (A.2) is obtained by switching to cylindric coordinates. With

$$\lambda_1 = \lambda \sin \theta \cos \varphi, \quad \lambda_2 = \lambda \sin \theta \sin \varphi, \quad \lambda_3 = \lambda \cos \theta$$

we can write:

$$\begin{aligned} \frac{\Theta_{ii}}{\sigma_Y^2 I_Y^2} &= \frac{2}{\pi^2} \int_0^\infty \int_0^\pi \int_0^{2\pi} \frac{F_{ii}(\lambda, \theta, \varphi) \exp(-4\pi\lambda^2) \sin \theta}{\sin^2 \theta \cos^2 \varphi + (4\pi^2/Pe^2)\lambda^2} \cdot \\ &\cdot \left\{ 1 + \exp\left[-\left(\frac{8\pi^2}{Pe}\lambda^2\right)\tau\right] - 2 \cos[(2\pi\lambda \sin \theta \cos \varphi)\tau] \times \right. \\ &\times \left. \exp\left[-\left(\frac{4\pi^2}{Pe}\lambda^2\right)\tau\right] \right\} d\varphi d\theta d\lambda \end{aligned} \quad (\text{A.3})$$

where

$$\begin{aligned} F_{11}(\lambda, \theta, \varphi) &= (1 - \sin^2 \theta \cos^2 \varphi)^2, & F_{22}(\lambda, \theta, \varphi) &= (\sin^2 \theta \sin \varphi \cos \varphi)^2, \\ F_{33}(\lambda, \theta, \varphi) &= (\sin \theta \cos \varphi \cos \theta)^2 \end{aligned} \quad (\text{A.4})$$

When $\tau \rightarrow 0$, Equation (A.3) yields:

$$\frac{\Theta_{ii}}{\sigma_Y^2 I_Y^2} = \frac{2Pe^2 \tau^2}{\pi^2} \int_0^\infty \int_0^\pi \int_0^{2\pi} \frac{F_{ii} \sin^3 \theta \cos^2 \varphi \exp(-4\pi \lambda^2) \lambda^2}{\lambda^2 + (Pe^2/4\pi^2) \sin^2 \theta \cos^2 \varphi} d\varphi d\theta d\lambda \quad (\text{A.5})$$

The integration over λ (Gradshteyn and Ryzhik, 1980) and the expansion for $Pe \rightarrow \infty$ lead to:

$$\frac{\Theta_{ii}}{\sigma_Y^2 I_Y^2} = \frac{\tau^2}{4\pi} \int_0^\pi \int_0^{2\pi} F_{ii} \sin \theta d\varphi d\theta \quad (\text{A.6})$$

It is easy to verify that the final solutions can be written as

$$\Theta_{11}(t) = \frac{8}{15} \sigma_Y^2 U^2 t^2, \quad \Theta_{22}(t) = \Theta_{33}(t) = \frac{1}{15} \sigma_Y^2 U^2 t^2 \quad (\text{A.7})$$

The singular behavior of the integrand function in (A.2) when $i = 1$ near the origin of the wavenumbers domain does not allow for a direct integration at large times. Thus, we will switch to the study of the two-particle moment rate of change. The time derivative of (A.3) is

$$\frac{d}{d\tau} \left(\frac{\Theta_{ii}}{\sigma_Y^2 I_Y^2} \right) = \frac{d^{(A)}}{d\tau} \left(\frac{\Theta_{ii}}{\sigma_Y^2 I_Y^2} \right) + \frac{d^{(B)}}{d\tau} \left(\frac{\Theta_{ii}}{\sigma_Y^2 I_Y^2} \right) + \frac{d^{(C)}}{d\tau} \left(\frac{\Theta_{ii}}{\sigma_Y^2 I_Y^2} \right) \quad (\text{A.8})$$

where

$$\begin{aligned} & \frac{d^{(A)}}{d\tau} \left(\frac{\Theta_{ii}}{\sigma_Y^2 I_Y^2} \right) \\ &= -\frac{4Pe}{\pi^2} \int_0^\infty \int_0^\pi \int_0^{2\pi} \frac{(F_{ii} \sin \theta) \exp[-(4\pi + (8\pi^2/Pe)\tau)\lambda^2]}{\lambda^2 + (Pe^2/4\pi^2) \sin^2 \theta \cos^2 \varphi} \lambda^2 d\varphi d\theta d\lambda \end{aligned} \quad (\text{A.9})$$

$$\begin{aligned} & \frac{d^{(B)}}{d\tau} \left(\frac{\Theta_{ii}}{\sigma_Y^2 I_Y^2} \right) \\ &= \frac{4Pe}{\pi^2} \int_0^\infty \int_0^\pi \int_0^{2\pi} \frac{(F_{ii} \sin \theta) \exp[-(4\pi + (4\pi^2/Pe)\tau)\lambda^2]}{\lambda^2 + (Pe^2/4\pi^2) \sin^2 \theta \cos^2 \varphi} \\ & \quad \cdot \cos[(2\pi \lambda \sin \theta \cos \varphi)\tau] \lambda^2 d\varphi d\theta d\lambda \end{aligned} \quad (\text{A.10})$$

$$\begin{aligned} & \frac{d^{(C)}}{d\tau} \left(\frac{\Theta_{ii}}{\sigma_Y^2 I_Y^2} \right) \\ &= \frac{2Pe^2}{\pi^3} \int_0^\infty \int_0^\pi \int_0^{2\pi} \frac{(F_{ii} \sin^2 \theta \cos \varphi) \exp[-(4\pi + (4\pi^2/Pe)\tau)\lambda^2]}{\lambda^2 + (Pe^2/4\pi^2) \sin^2 \theta \cos^2 \varphi} \times \\ & \quad \times \sin[(2\pi \lambda \sin \theta \cos \varphi)\tau] \lambda d\varphi d\theta d\lambda \end{aligned} \quad (\text{A.11})$$

The integration of (A.9), (A.10) and (A.11) over λ (Gradstheyn and Ryzhik, 1980) gives

$$\begin{aligned} \frac{d}{d\tau} \left(\frac{\Theta_{ii}}{\sigma_Y^2 I_Y^2} \right) &= \frac{4Pe}{\pi^2} \int_0^\pi \int_0^{2\pi} F_{ii} \sin \theta \left\{ \frac{\sqrt{\pi}}{2\sqrt{\beta'}} + \frac{\sqrt{\pi}}{2\sqrt{\beta}} \exp \left(-\frac{\alpha^2}{4\beta} \right) + \right. \\ &\quad \left. + \frac{\pi\gamma}{2} \exp \left(\beta'\gamma^2 \right) \left[\Phi \left(\gamma\sqrt{\beta} + \frac{\alpha}{2\sqrt{\beta}} \right) - \Phi \left(\gamma\sqrt{\beta'} \right) \right] \right\} d\varphi d\theta \end{aligned} \tag{A.12}$$

where $\alpha = 2\pi\tau \sin \theta \cos \varphi$, $\beta = 4\pi + (4\pi^2\tau)/Pe$, $\beta' = 2\beta - 4\pi$, $\gamma = (Pe \sin \theta \cos \varphi)/2\pi$, and $\Phi(\cdot)$ indicates the Error Function.

At large time, for finite Peclet ($\tau/Pe = \tau' \rightarrow \infty$), the expansion of the integrand function produces

$$\begin{aligned} \frac{d}{d\tau} \left(\frac{\Theta_{ii}}{\sigma_Y^2 I_Y^2} \right) &= \frac{Pe}{3\pi^{5/2}\sqrt{\tau'}} \int_0^\pi \int_0^{2\pi} (F_{ii} \sin \theta) \times \\ &\quad \times \exp \left[-\left(\frac{Pe^2}{4} \cos^2 \varphi \sin^2 \theta \right) \tau' \right] d\varphi d\theta \end{aligned} \tag{A.13}$$

Furthermore, when $\tau' \rightarrow \infty$,

$$\exp \left[-\left(\frac{Pe^2}{4} \cos^2 \varphi \sin^2 \theta \right) \tau' \right] \rightarrow 2\sqrt{\pi}/(Pe\sqrt{\tau'})\delta(\cos \varphi \sin \theta)$$

Thus,

$$\frac{d}{d\tau} \left(\frac{\Theta_{11}}{\sigma_Y^2 I_Y^2} \right) \rightarrow \frac{8}{3\pi^2\tau'} \quad \Theta_{11} \rightarrow \frac{8Pe}{3\pi^2}\sigma_Y^2 I_Y^2 \ln \left(\frac{tU}{I_Y} \right) + \text{const} \tag{A.14}$$

$$\frac{d}{d\tau} \left(\frac{\Theta_{22}}{\sigma_Y^2 I_Y^2} \right) \rightarrow 0 \quad \Theta_{22} \rightarrow \text{const} \tag{A.15}$$

$$\frac{d}{d\tau} \left(\frac{\Theta_{33}}{\sigma_Y^2 I_Y^2} \right) \rightarrow 0 \quad \Theta_{33} \rightarrow \text{const} \tag{A.16}$$

The constant asymptotic values of Θ_{22} and Θ_{33} are found from (A.3):

$$\begin{aligned} \frac{\Theta_{ii}}{\sigma_Y^2 I_Y^2} &= \frac{2}{\pi^2} \int_0^\infty \int_0^\pi \int_0^{2\pi} \frac{(F_{ii} \sin \theta) \exp(-4\pi\lambda^2)}{\sin^2 \theta \cos^2 \varphi + (4\pi^2/Pe^2)\lambda^2} d\varphi d\theta d\lambda \\ &= \frac{Pe^2}{2\pi^4} \int_0^\infty \int_0^\pi \int_0^{2\pi} \frac{(F_{ii} \sin \theta) \exp(-4\pi\lambda^2)}{\lambda^2 + (Pe^2/4\pi^2) \sin^2 \theta \cos^2 \varphi} d\varphi d\theta d\lambda \end{aligned} \tag{A.17}$$

For large Peclet numbers (Gradstheyn and Ryzhik, 1980):

$$\int_0^\infty \frac{\exp(-4\pi\lambda^2)}{\lambda^2 + (Pe^2/4\pi^2) \sin^2 \theta \cos^2 \varphi} d\lambda \rightarrow \frac{\pi^2}{Pe^2 \sin^2 \theta \cos^2 \varphi}$$

and

$$\frac{\Theta_{ii}}{\sigma_Y^2 l_Y^2} = \frac{1}{2\pi^2} \int_0^\pi \int_0^{2\pi} \frac{F_{ii}}{\sin \theta \cos^2 \varphi} d\varphi d\theta \quad (\text{A.18})$$

Finally, the integration over φ and θ leads to

$$\Theta_{22} = \Theta_{33} = \frac{2}{3\pi} \sigma_Y^2 l_Y^2 \quad (\text{A.19})$$

Appendix B.

For the computation of the spectral density of Y in case of isotropic hole–Gaussian covariances we will refer to (e.g. Dagan, 1989):

$$S_Y(k)_{k=|k|} = \frac{2}{k} \int_0^\infty C_Y(r) \sin(2\pi kr) r dr \quad (\text{A.20})$$

obtained from

$$S_Y(k)_{k=|k|} = \int_{\mathbf{r}} C_Y(r) \exp(-j2\pi \mathbf{k} \cdot \mathbf{r}) d\mathbf{r}$$

by switching to cylindric coordinates, with $\cos(2\pi kr)r^2 \simeq \sin(2\pi kr)/(2\pi k)r$ for $r \rightarrow 0$ (that is, for the interval of r -values which give the maximum contribution in terms of $C_Y(r)$). Thus, from (38), we obtain:

$$S_Y(\lambda)_{\lambda=|\lambda|} = \frac{4}{3} \pi^3 \sqrt{2\pi} \sigma_Y^2 l^3 \lambda^2 \exp(-2\pi^2 \lambda^2) \quad (\text{A.21})$$

Note that, in this case, the dimensionless groups are $\lambda_i = k_i l$, $\tau = tU/l$ and $Pe = Ul/D$.

From (25), (26) and (A.21), for $\tau \rightarrow 0$ we obtain:

$$\begin{aligned} & \frac{\Theta_{ii}}{\sigma_Y^2 l^2} \\ &= \frac{4\pi^3 \sqrt{2\pi} \tau^2}{3} \int_0^\infty \int_0^\pi \int_0^{2\pi} \frac{F_{ii} \sin^3 \theta \cos^2 \varphi \exp(-2\pi^2 \lambda^2) \lambda^4}{\sin^2 \theta \cos^2 \varphi + (4\pi^2/Pe^2) \lambda^2} d\varphi d\theta d\lambda \end{aligned} \quad (\text{A.22})$$

In case of large Peclet numbers, the triple integral (Gradshteyn and Ryzhik, 1980) gives, at the leading order

$$\Theta_{11}(t) = \frac{4}{15} \sigma_Y^2 U^2 t^2, \quad \Theta_{22}(t) = \Theta_{33}(t) = \frac{1}{30} \sigma_Y^2 U^2 t^2 \quad (\text{A.23})$$

In order to derive the large-time longitudinal two-particle moment, we will first integrate in the wavenumbers rectangular domain:

$$\begin{aligned} \frac{\Theta_{11}}{\sigma_Y^2 l^2} &= \frac{\pi \sqrt{2\pi}}{3} \int_{-\infty}^\infty \int_{-\infty}^\infty \int_{-\infty}^\infty \left(1 - \frac{\lambda_1^2}{\lambda_1^2 + \lambda_2^2 + \lambda_3^2} \right)^2 \\ &\cdot \frac{(\lambda_1^2 + \lambda_2^2 + \lambda_3^2) \exp[-2\pi^2(\lambda_1^2 + \lambda_2^2 + \lambda_3^2)]}{\lambda_1^2 + (4\pi^2/Pe^2)(\lambda_1^2 + \lambda_2^2 + \lambda_3^2)^2} d\lambda_1 d\lambda_2 d\lambda_3 \end{aligned} \quad (\text{A.24})$$

With $v_1 = \lambda_1/(2\pi/Pe)$ and $Pe \rightarrow \infty$,

$$\frac{\Theta_{11}}{\sigma_Y^2 l^2} = \frac{\sqrt{2\pi}}{6} Pe \int_{-\infty}^{\infty} \int_{-\infty}^{\infty} \int_{-\infty}^{\infty} \frac{(\lambda_2^2 + \lambda_3^2) \exp[-2\pi^2(\lambda_2^2 + \lambda_3^2)]}{v_1^2 + (\lambda_2^2 + \lambda_3^2)^2} dv_1 d\lambda_2 d\lambda_3 \quad (\text{A.25})$$

The integration over v_1 is easily performed resorting to the following formula (Gradshteyn and Ryzhik, 1980):

$$\int_{-\infty}^{\infty} \frac{1}{v_1^2 + (\lambda_2^2 + \lambda_3^2)^2} dv_1 = \frac{\pi}{\lambda_2^2 + \lambda_3^2}$$

Then,

$$\frac{\Theta_{11}}{\sigma_Y^2 l^2} = \frac{\pi\sqrt{2\pi}}{6} Pe \int_{-\infty}^{\infty} \int_{-\infty}^{\infty} \exp[-2\pi^2(\lambda_2^2 + \lambda_3^2)] d\lambda_2 d\lambda_3$$

Finally, the integration over λ_2 and λ_3 is transformed into an integration in the polar domain (λ, ϑ) :

$$\frac{\Theta_{11}}{\sigma_Y^2 l^2} = \frac{\pi\sqrt{2\pi}}{6} Pe \int_0^{\infty} \int_0^{2\pi} \exp(-2\pi^2\lambda^2)\lambda d\vartheta d\lambda$$

The result is

$$\Theta_{11} = \frac{\sqrt{\pi} Pe}{6\sqrt{2}} \sigma_Y^2 l^2 \quad (\text{A.26})$$

Along the transverse direction, in the cylindric reference frame and at leading order for $Pe \rightarrow \infty$:

$$\frac{\Theta_{22}}{\sigma_Y^2 l^2} = \frac{\pi\sqrt{2\pi}}{3} \int_0^{\infty} \int_0^{\pi} \int_0^{2\pi} \sin^3 \theta \sin^2 \varphi \exp(-2\pi^2\lambda^2)\lambda^2 d\varphi d\theta d\lambda \quad (\text{A.27})$$

The integrations over φ , θ and λ are easy and independent. The final result is

$$\Theta_{22} = \frac{1}{18} \sigma_Y^2 l^2 \quad (\text{A.28})$$

The procedure for Θ_{33} is identical and, due to the isotropy of the log-conductivity field, leads to the same result:

$$\Theta_{33} = \frac{1}{18} \sigma_Y^2 l^2 \quad (\text{A.29})$$

Appendix C.

In order to evaluate the asymptotic macrodispersion coefficients for the first-type hole–Gaussian log-conductivity covariance, we will use the same method applied

by Gelhar and Axness (1983). Since in the present work the Fourier transforms are defined as

$$F(\mathbf{k}) = \int_{\mathbf{x}} f(\mathbf{x}) \exp(-j2\pi \mathbf{k} \cdot \mathbf{x}) d\mathbf{x}$$

their expression (22') becomes:

$$D_{mii} = UA_{ii} = \int_{-\infty}^{\infty} \int_{-\infty}^{\infty} \int_{-\infty}^{\infty} \frac{(4\pi^2 D \sum_r \lambda_r^2 / l^2) S_{iii}(\lambda_1, \lambda_2, \lambda_3)}{(2\pi \lambda_1 U / l)^2 + (4\pi^2 D \sum_r \lambda_r^2 / l^2)^2} \times \frac{d\lambda_1 d\lambda_2 d\lambda_3}{l^3} \quad (\text{A.30})$$

Thus, for the log-K spectrum (74):

$$\frac{D_{mii}}{\sigma_Y^2 D} = \frac{4\pi^3 \sqrt{2\pi}}{3} \int_{-\infty}^{\infty} \int_{-\infty}^{\infty} \int_{-\infty}^{\infty} \times \frac{F_{ii}(\lambda_1^2 + \lambda_2^2 + \lambda_3^2)^2 \exp[-2\pi^2(\lambda_1^2 + \lambda_2^2 + \lambda_3^2)]}{\lambda_1^2 + (4\pi^2 / Pe^2)(\lambda_1^2 + \lambda_2^2 + \lambda_3^2)^2} d\lambda_1 d\lambda_2 d\lambda_3$$

The longitudinal coefficient will be found through

$$\frac{D_{m11}}{\sigma_Y^2 D} = \frac{4\pi^3 \sqrt{2\pi}}{3} \int_{-\infty}^{\infty} \int_{-\infty}^{\infty} \int_{-\infty}^{\infty} \left(1 - \frac{\lambda_1^2}{\lambda_1^2 + \lambda_2^2 + \lambda_3^2}\right)^2 \cdot \frac{(\lambda_1^2 + \lambda_2^2 + \lambda_3^2)^2 \exp[-2\pi^2(\lambda_1^2 + \lambda_2^2 + \lambda_3^2)]}{\lambda_1^2 + (4\pi^2 / Pe^2)(\lambda_1^2 + \lambda_2^2 + \lambda_3^2)^2} d\lambda_1 d\lambda_2 d\lambda_3 \quad (\text{A.31})$$

The substitution $v_1 = \lambda_1 / (2\pi / Pe)$ when $Pe \rightarrow \infty$ yields

$$\frac{D_{m11}}{\sigma_Y^2 D} = \frac{2\pi^2 \sqrt{2\pi}}{3} Pe \int_{-\infty}^{\infty} \int_{-\infty}^{\infty} \int_{-\infty}^{\infty} \frac{(\lambda_2^2 + \lambda_3^2)^2 \exp[-2\pi^2(\lambda_2^2 + \lambda_3^2)]}{v_1^2 + (\lambda_2^2 + \lambda_3^2)^2} \times dv_1 d\lambda_2 d\lambda_3$$

and, finally,

$$D_{m11} = \frac{1}{6} \sqrt{2\pi} \sigma_Y^2 U l \quad (\text{A.32})$$

For the transverse coefficient, switching to cylindrical coordinates, and at leading order for $Pe \rightarrow \infty$:

$$\frac{D_{m22}}{\sigma_Y^2 D} = \frac{4}{3} \pi^3 \sqrt{2\pi} \int_0^\infty \int_0^\pi \int_0^{2\pi} \sin^3 \theta \sin^2 \varphi \exp(-2\pi^2 \lambda^2) \lambda^4 d\varphi d\theta d\lambda$$

and

$$D_{m22} = D_{m33} = \frac{1}{6} \sigma_Y^2 D \quad (\text{A.33})$$

References

- Batchelor, G. K.: 1952, Diffusion in a field of homogeneous turbulence, 2, The relative motion of particles, *Proc. Cambridge Philos. Soc.* **48**, 345–362.
- Bellin, A., Salandin, P. and Rinaldo, A.: 1992, Simulation of dispersion in heterogeneous porous formations: statistics, first-order theories, convergence of computations, *Water Resour. Res.* **28**(9), 2211–2227.
- Dagan, G.: 1984, Solute transport in heterogeneous porous formations, *J. Fluid Mech.* **145**, 151–177.
- Dagan, G.: 1989, *Flow and Transport in Porous Media*, Springer, Berlin, 465 pp.
- Dagan, G.: 1990, Transport in heterogeneous porous formations: spatial moments, ergodicity, and effective dispersion, *Water Resour. Res.* **26**(6), 1281–1290.
- Dagan, G.: 1991, Dispersion of a passive solute in non-ergodic transport by steady velocity fields in heterogeneous formations, *J. Fluid Mech.* **223**, 197–210.
- Dagan, G.: 1994, The significance of heterogeneity of evolving scales and of anomalous diffusion to the transport in porous formations, *Water Resour. Res.* **30**(12), 3327–3336.
- Dentz, M., Kinzelbach, H., Attinger, S. and Kinzelbach, W.: 2000a, Temporal behavior of a solute cloud in a heterogeneous porous medium, 1, Point-like injection, *Water Resour. Res.* **36**(12), 3591–3604.
- Dentz, M., Kinzelbach, H., Attinger, S. and Kinzelbach, W.: 2000b, Temporal behavior of a solute cloud in a heterogeneous porous medium, 2, Spatially extended injection, *Water Resour. Res.* **36**(12), 3605–3614.
- Fiori, A.: 1996, Finite Peclet extensions of Dagan's solution to transport in anisotropic heterogeneous formations, *Water Resour. Res.* **32**(1), 193–198.
- Fiori, A. and Dagan, G.: 2000, Concentration fluctuations in aquifer transport: a rigorous first-order solution and applications, *J. Contam. Hydrol.* **45**(3–4), 139–163.
- Fisher, H. B., List, E. J., Koh, R. C. Y., Imberger, J. and Brooks, N. H.: 1979, *Mixing in Inland and Coastal Waters*, Academic, San Diego, CA, 483 pp.
- Garabedian, S. P., Leblanc, D. R., Gelhar, L. W. and Celia, M. A.: 1991, Large-scale natural gradient tracer test in sand and gravel, Cape-Cod, Massachusetts, 2, Analysis of spatial moments for a nonreactive tracer, *Water Resour. Res.* **27**(5), 911–924.
- Gelhar, L. W.: 1997, *Stochastic Subsurface Hydrology*, Prentice-Hall, Englewood Cliffs, NJ.
- Gelhar, L. W. and Axness, C. L.: 1983, Three-dimensional stochastic analysis of macrodispersion in aquifers, *Water Resour. Res.* **19**(1), 161–180.
- Gradshcheyn, I. S. and Ryzhik, I. M.: 1980, *Table of Integral, Series, and Products, 5th edn*, Academic Press, San Diego, CA, 1204 pp.
- Güven, O., Molz, F. J. and Melville, J. G.: 1984, An analysis of dispersion in a stratified aquifer, *Water Resour. Res.* **20**(10), 1337–1354.
- Hess, K. M., Wolf, S. H. and Celia, M. A.: 1991, Large-scale natural gradient tracer test in sand and gravel, Cape-Cod, Massachusetts, 3, Hydraulic conductivity variability and calculated macrodispersivity, *Water Resour. Res.* **27**(5), 2011–2027.
- Kapoor, V. and Gelhar, L. W.: 1994a, Transport in three-dimensionally heterogeneous aquifers: 1. Dynamics of concentration fluctuations, *Water Resour. Res.* **30**(6), 1775–1788.
- Kapoor, V. and Gelhar, L. W.: 1994b, Transport in three-dimensionally heterogeneous aquifers: 2. Predictions and observations of concentration fluctuations, *Water Resour. Res.* **30**(6), 1789–1801.
- Kapoor, V. and Kitanidis, P. K.: 1998, Concentration fluctuations and dilution in aquifers, *Water Resour. Res.* **34**(5), 1181–1193.
- Kitanidis, P. K.: 1988, Prediction by the method of moments of transport in a heterogeneous formation, *J. Hydrol.* **102**, 453–473.
- Kitanidis, P. K.: 1992, An analysis of macrodispersion through volume-averaging: Moments equations, *Stochastic Hydrol. Hydraul.* **6**, 5–25.
- Leblanc, D. R., Garabedian, S. P., Hess, K. M., Gelhar, L. W., Quadri, R. D., Stollenwerk, K. G. and Wood, W. W.: 1991, Large-scale natural gradient tracer test in sand and gravel, Cape-Cod,

- Massachusetts, 1, Experimental design and observed tracer movement, *Water Resour. Res.* **27**(5), 895–910.
- Neuman, S. P., Winter, C. L. and Newman, C. M.: 1987, Stochastic theory of field-scale Fickian dispersion in anisotropic porous media, *Water Resour. Res.* **23**(3), 453–466.
- Pannone, M. and Kitanidis, P. K.: 1999, Large-time behavior of concentration variance and dilution in heterogeneous formations, *Water Resour. Res.* **35**(3), 623–634.
- Pannone, M. and Kitanidis, P. K.: 2001, Large-time spatial structure of concentration of conservative solute and application to the Cape Cod tracer test, *Transport Porous Med.* **42**(1/2), 109–132.
- Rajaram, H. and Gelhar, L. W.: 1993, Plume scale-dependent dispersion in heterogeneous aquifers 2. Eulerian analysis and three-dimensional aquifers, *Water Resour. Res.* **29**(9), 3261–3276.
- Rubin, Y.: 1990, Stochastic modeling of macrodispersion in heterogeneous porous media, *Water Resour. Res.* **26**(1), 133–141.
- Rubin, Y.: 2003, *Applied Stochastic Hydrogeology*, Oxford University Press, 288 pp.
- Vomvoris, E. G. and Gelhar, L. W.: 1990, Stochastic analysis of the concentration variability in a three-dimensional heterogeneous aquifer, *Water Resour. Res.* **26**(10), 2591–2602.
- Zhang, Y.-K. and Di Federico, V.: 1998, Solute transport with a Gaussian covariance of log hydraulic conductivity, *Water Resour. Res.* **34**(8), 1929–1934.